

## **Integrated Photonic Devices and Materials Group**

### **Academic and Research Staff**

Professor Leslie A. Kolodziejski, Dr. Gale S. Petrich, Principal Research Scientist

### **Graduate Students**

Mohammad Araghchini, Reginald E. Bryant, Peichun (Amy) Chi, Natalija Jovanović, Sheila Nabanja, Orit Shamir, Ta-Ming Shih

### **Technical and Support Staff**

Tiffany Kuhn, Denise Stewart

### **Introduction**

The emphasis of our research program is the design, epitaxial growth, device fabrication and characterization of a number of photonic and opto-electronic structures and devices. The epitaxial growth of the heterostructures is performed in a Veeco GEN 200 solid source, multi-wafer, dual-reactor molecular beam epitaxy (MBE) system. The Veeco MBE system is capable of the epitaxial growth of dilute nitrides and antimony-based films in addition to arsenide- and phosphide-based films.

In the following sections, the status of the various research projects will be discussed. Projects include the development and simulation of rudimentary optical logic gates, the development of optical modulators for operation at 800nm, the development of Si-based two-dimensional photonic crystal super-collimators, the development of semiconductor lasers with novel active regions and the development of high index contrast optical switches. These projects are collaborative efforts of multiple professors at MIT and members of the MIT Lincoln Laboratory technical staff in order to successfully design, simulate, fabricate and characterize the aforementioned optical devices.

## **1. Photonic Integrated Circuits for Ultrafast Optical Logic**

### **Sponsors**

Defense Advanced Research Projects Agency: Contract Number: W911NF-06-1-0060

Defense Advanced Research Projects Agency: Contract Number: W911NF-07-1-0630

### **Project Staff**

Ta-Ming Shih, Ryan D. Williams, Dr. Gale S. Petrich, Professor Rajeev Ram, Professor Erich P. Ippen, and Professor Leslie A. Kolodziejski

The aim of this project is to model and to produce a modular, monolithically-integrated, all-optical unit cell capable of performing a complete set of Boolean operations at speeds of hundreds of gigabits per second. Optical logic operations, wavelength conversion, and other advanced optical switching schemes can be implemented using this basic unit cell which consists of a balanced Mach-Zehnder interferometer with an InGaAsP-based semiconductor optical amplifier in each arm. Device design and fabrication tolerances were analyzed using the beam propagation method and finite-difference time-domain techniques prior to fabrication.

Complete optical logic structures have been fabricated using the twin waveguide approach which vertically couples the passive waveguides and the active amplifiers. Using an adiabatic taper coupler, the optical mode is transferred between the lower passive waveguide and the upper active waveguide of the twin-waveguide structure, as seen in Figure 1. The passive waveguides have a measured loss of 0.89dB/cm. Diode characteristics have been measured for the SOAs as well. Currently, the effort is to improve upon the fabricated structures in order to lower the contact resistance and to improve the planarization uniformity across the chip. A new contact metal mask has been designed to improve the current injection and to allow for easier probing of the SOAs.

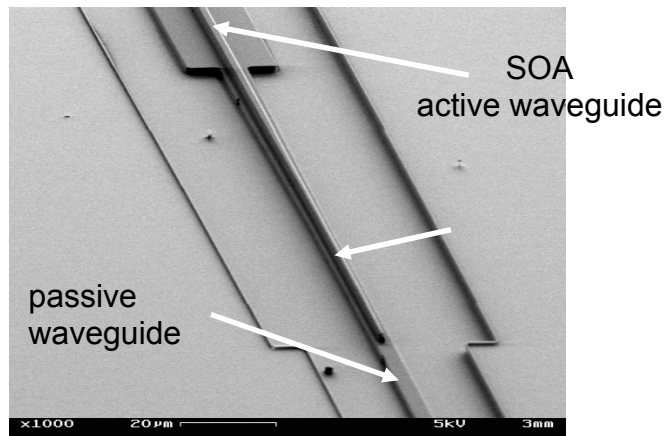


**Figure 1)** A scanning electron micrograph showing the active waveguide taper that is used to transfer the optical mode between the lower passive waveguide (lower right) and the upper active waveguide (upper left).

## 2. Ultra Broad Band Modulator Arrays

### Sponsors

Defense Advanced Research Projects Agency: Contract Number: HR0011-05-C-0155

### Project Staff

Orit Shamir, Dr. Gale S. Petrich, Professor Franz X. Kaertner, Professor Erich P. Ippen and Professor Leslie A. Kolodziejski

To create an arbitrary optical waveform at wavelengths that are centered at 800nm, ultra broad band modulator arrays are required. Since these modulators are to operate around 800nm, the material choices are limited to relatively high Al content AlGaAs and to  $\text{In}_{0.5}(\text{Ga}_x\text{Al}_{1-x})_{0.5}\text{P}$  layers that are lattice-matched to GaAs. In addition, since GaAs absorbs light with a wavelength less than 870nm, the lower cladding layer of the modulator must be relatively thick in order to isolate the modulator from the GaAs substrate. To create the largest mode possible and to minimize the coupling loss, the index contrast between the waveguiding layers and the cladding layers should be minimized. To minimize the index contrast, a dilute waveguide structure in which thin layers of high index material are embedded in a low index material is employed. The resulting layered structure has an effective index slightly higher than the low index material and is determined by the layer thicknesses as well as the refractive index of the two materials that comprise the dilute waveguide.

The modular structure that was grown by molecular beam epitaxy is an  $\text{Al}_{0.8}\text{Ga}_{0.2}\text{As}$ -based structure in which the dilute waveguide consists of alternating layers of  $\text{Al}_{0.8}\text{Ga}_{0.2}\text{As}$  and InGaP. The structure is challenging in terms of the epitaxial growth. Although the use of  $\text{Al}_{0.8}\text{Ga}_{0.2}\text{As}$  for the cladding layer minimized the lattice-mismatch problem, achieving high quality, high Al content AlGaAs cladding layers is difficult due to the low Al adatom mobility on the surface during growth. To minimize free carrier loss, P-I-N structures are employed in which the Si and Be dopants are graded from the contact layers to the dilute waveguide region. Photoluminescence (PL) measurements from the arsenide-based structure show a weak PL peak at ~650nm from the InGaP layers in the dilute waveguide. The  $\text{Al}_{0.8}\text{Ga}_{0.2}\text{As}$  and  $\text{Al}_{0.5}\text{Ga}_{0.5}\text{As}$  layers as well as the InAlP layers have indirect band gaps and hence do not exhibit photoluminescence. Due to the high etch selectivity between the arsenide and phosphide layers, the uppermost high index layer of the dilute waveguide also acts as an etch stop.

In addition to this original structure, a second Metal-Oxide-Semiconductor-type structure has also been grown which differs from the previous design by the addition of two oxidized AIAs layers, enabling a strongly confined optical mode in the middle of the structure. The  $\text{Al}_x\text{O}_y$  layers will allow the device to be capable of withstanding higher operating voltages. Furthermore, the device can be unipolar. The structure also contains an InAIP etch stop to facilitate fabrication.

The optical properties of the dilute waveguide in both structures have been simulated using OptiBPM (Optiwave Corporation). The  $\text{Al}_{0.8}\text{Ga}_{0.2}\text{As}$ -based structure is designed to support a single optical mode within a 2 micron wide ridge waveguide; the fundamental mode for the arsenide-based structure is roughly  $2\mu\text{m} \times 1\mu\text{m}$  (W x H). The MOS-type structure is also designed to support a single optical mode, which is roughly  $1.5\mu\text{m} \times 1\mu\text{m}$  (W x H) as simulated by OptiBPM. If the dilute waveguide of the  $\text{Al}_{0.8}\text{Ga}_{0.2}\text{As}$ -based structure is not completely etched, due to the low index contrast of the dilute waveguide, the bending radius is quite large, on the order of a millimeter. Ultimately, the modulator will be incorporated into an array waveguide grating, therefore the loss needs to be considered.

A new self-aligned fabrication process, which defines both the passive devices and the powered modulators in the same step, has been developed that is compatible with both the MOS-type structure and the  $\text{Al}_{0.8}\text{Ga}_{0.2}\text{As}$ -based design. The only difference in the fabrication process is the addition of the AIAs oxidation step that is inserted after the reactive ion etching that is used to define the waveguides. The mask set associated with this process has been designed and fabricated. The mask set contains Mach Zehnder interferometer modulators of various lengths with multimode interference couplers or Y-splitters. The Mach Zehnder interferometer modulators as well as conventional modulators are oriented both parallel and perpendicular to the major flat of the 2" GaAs (100) wafers. The mask set also contains a variety of passive components such as Y-splitters, multimode interference couplers as well as straight and curved waveguides. Figure 1 shows the waveguide of the AlGaAs-based design that was reactive-ion-etched using a HBr-plasma.

Arbitrary waveform generation is obtained by the phase and amplitude modulation of the individual frequency components within a frequency comb. Hence, optical wavelength demultiplexers and multiplexers are necessary for the spatial separation and recombination of wavelength components prior to and following modulation. Therefore, the structure and performance of arrayed waveguide gratings (AWG) have been modeled and a mask containing the AWG is currently being designed. The AWG has eight input and output waveguides that are each  $2\mu\text{m}$  wide. As the input aperture of the free propagation region (FPR) is approached, the waveguide width gradually increases to  $3\mu\text{m}$  over a length of  $50\mu\text{m}$ . The output waveguides taper in width at the output aperture, scaling back from  $3\mu\text{m}$  to  $2\mu\text{m}$  over a similar length. Adjusting the waveguide width, allows the optical mode to smoothly transition from the confined waveguides to the dispersive free propagation region. The thirty waveguides in the phased array section similarly taper from a width of  $4\mu\text{m}$  to  $3\mu\text{m}$ . At the first FPR output, where the waveguides are  $4\mu\text{m}$  wide, there is no space between the waveguides, encouraging full transmission of the diffracted power from the first FPR to the phased array waveguides and on to the second FPR. The AWG is designed and simulated to have 10 GHz channel spacing with -30dB to -40dB of optical cross-talk between output waveguides.

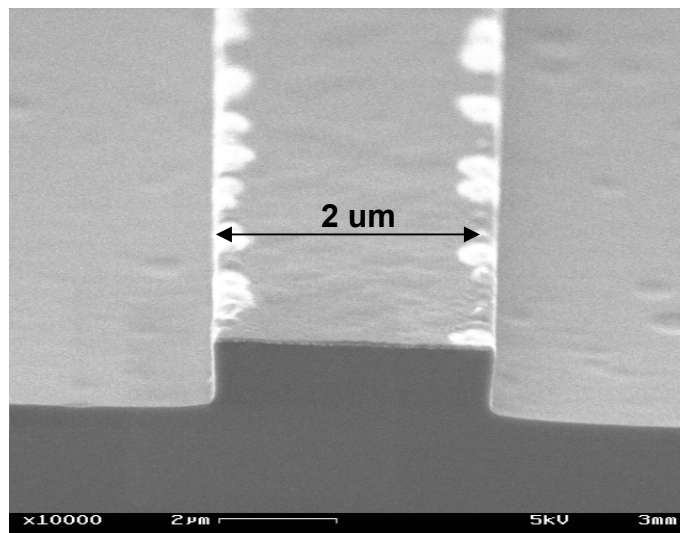


**Figure 1)** Scanning electron micrograph of an etched passive ridge of the  $\text{Al}_{0.8}\text{Ga}_{0.2}\text{As}$  and  $\text{InGaP}$  P-I-N structure for waveguide loss measurements.

### 3. Super-collimation of Light within Photonic Crystal Slabs

#### Sponsor

National Science Foundation Award Number DMR-02-13282

MARCO Interconnect Focus Center, Subcontract from Georgia Institute of Technology  
Contract Number B-12-M06-52

Wide Net Technology Award Number: 014-337-001

#### Project Staff

Andre Kurs, Ta-Ming Shih, Marcus Dahlem, Dr. Gale S. Petrich, Professor Marin Soljacic, Professor Erich P. Ippen, Professor Leslie A. Kolodziejcki, Dr. Katherine Hall and Dr. Morris Kessler

Super-collimation (SC) is the propagation of light without diffraction using the intrinsic properties of photonic crystals (PhCs). Successful fabrication and measurement of SC have been achieved for planar PhCs composed of silicon rods as well as air holes etched into silicon. The super-collimating PhC is fabricated on a silicon-on-insulator (SOI) wafer. The low-index  $\text{SiO}_2$  layer is used to minimize radiation loss into the high-index silicon substrate. The rods are defined using interference lithography and pattern transfer is achieved using reactive ion etching (RIE). Infrared images of the light that is scattered normal to the plane of the super-collimator that is composed of Si-rods on a SOI wafer are shown in Figure 1. Super-collimation is observed at a wavelength of 1530nm.

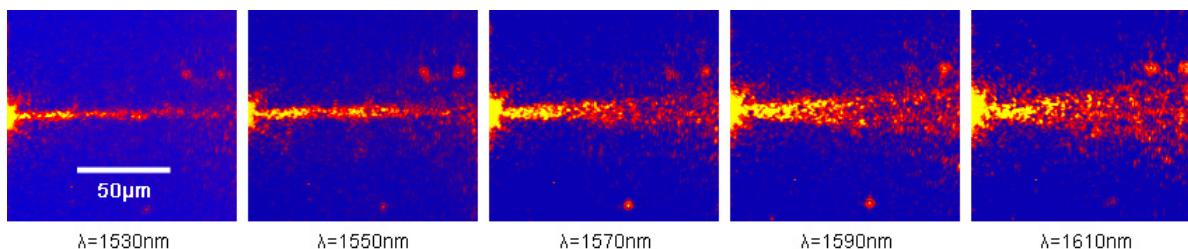


**Figure 1)** Plan-view infrared images showing the wavelength dependence of the propagating beam inside the two-dimensional-slab PhC that is composed of Si rods. The optimal wavelength of SC is close to 1530nm and the beam diverges for non-optimal wavelengths.

In principle, creating a beam which does not diverge for long distances is possible by making the distribution of the beam's constituent eigenmodes sufficiently narrow in k-space, i.e. as the beam approaches a single Bloch mode or plane wave. On the other hand, a super-collimator allows for nearly divergent-less propagation for beam widths only a few times the lattice constant of the PhC. A method of exploring the design space for super-collimating devices has been developed, and is shown in Figure 2, which plots the SC length as a function of wavelength and initial beam width for PhCs that are composed of Si rods as well as PhCs that are composed of air holes in a Si slab. As shown in Figure 2, the bandwidth for super-collimation for the photonic crystal of holes is wider than the bandwidth for that of rods. Hence, depending on the application, a photonic crystal that is composed of air holes may be more suitable than a photonic that is composed of dielectric rods.

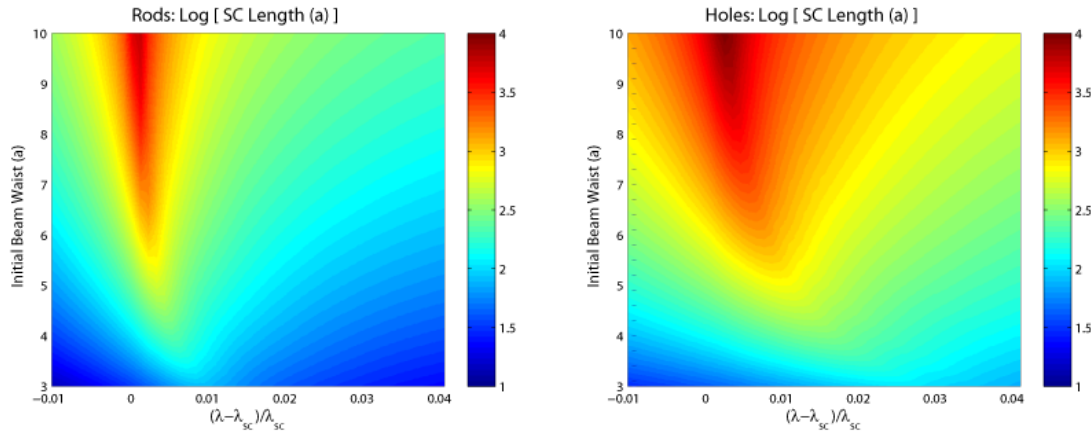


**Figure 2)** The logarithm of the super collimation length as a function of initial beam waist and wavelength, for a PhC (left) that is composed of a square lattice of silicon rods in air on SiO<sub>2</sub> (with dimensions  $a = 437.5\text{nm}$ ,  $r = 125\text{nm}$ , and  $h = 700\text{nm}$ ), for which the super-collimating modes are TM-like, and a PhC (right) that is composed of a square lattice of air holes in silicon on SiO<sub>2</sub> (with dimensions  $a = 350\text{nm}$ ,  $r = 105\text{nm}$ , and  $h = 205\text{nm}$ ), for which the super-collimating modes are TE-like.

#### 4. Electrically-Activated Nanocavity Laser using One-Dimensional Photonic Crystals

##### Sponsors

National Science Foundation: Award Number DMR-02-13282

##### Project Staff

Sheila Nabanja, Dr. Gale S. Petrich, and Professor Leslie A. Kolodziejski

Quantum-dot (QD) heterostructure lasers are a type of semiconductor laser that utilize quantum dots as the active media within the light-emitting region. Quantum dots are semiconductor nanocrystals of narrow band-gap material that are embedded in a wider band-gap material. The use of molecular beam epitaxy for the growth of highly lattice-mismatched III-V semiconductor materials has made the self-assembly of these structures possible. Due to the strong three-dimensional carrier confinement, devices that employ quantum dots have unique capabilities that are otherwise practically unachievable with bulk semiconductors, or even with quantum well structures.

One of the significant benefits of exploiting quantum effects in QD semiconductor lasers is to achieve lower threshold current densities. A reduction in the threshold current density is a direct result of the reduction in the translational degrees of freedom of the charge carriers (electrons and holes) thereby leading to an increase in the density of states of the charge carriers near the band edges. Another important benefit is that the threshold current density in QD lasers is unaffected by temperatures up to

about 300K since the carriers can only be thermally excited to a very limited number of these well-spaced energy levels within the quantum dots.

The goal of this work is to design and fabricate semiconductor lasers with novel quantum dot layers in the active region. The use of a separate confinement heterostructure will allow for electrical confinement while optical confinement will be achieved by means of ridge waveguides and index contrast. The semiconductor laser consists of epitaxially-grown layers of both doped and undoped semiconductor on n-GaAs substrate (Figure 1).

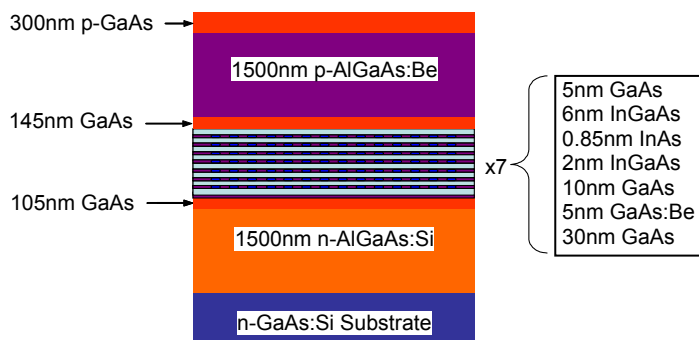


**Figure 1)** Structure of a semiconductor laser (sample VA55) with an active region consisting of seven  $\text{In}_{0.15}\text{Ga}_{0.85}\text{As}$  quantum wells with embedded  $\text{InAs}$  quantum dots and  $\text{Al}_{0.34}\text{Ga}_{0.66}\text{As}$  cladding layers.

In order to determine the etch depths that will yield the most single-mode lasers from the available mask-defined ridge widths, optical simulations have been performed using Optiwave's beam propagation software. The simulations have been carried out for ridge widths of  $1.5\mu\text{m}$  to  $30\mu\text{m}$  and ridge depths ranging from  $0.05\mu\text{m}$  to  $1.45\mu\text{m}$  for the laser structure that is shown in Figure 1.

Ridge waveguide lasers from sample VA55 are currently near completion. The front-end fabrication processes have included photolithography to define etch masks, a reactive ion etch and a wet etch of the arsenide-based material to create the ridges, a planarization step and then finally ohmic contact patterning. The remaining back-end processing includes lapping and metal evaporation.

Work has been done in determining a repeatable method to mount, lap and dismount wafers without introducing any damage to fully-processed devices. This work has included determining the bonding wax and grit size to use during lapping as well as establishing a reliable lapping technique.

Ultimately, the lasers will require characterization and to that end, a characterization setup has been designed. A laser diode driver will feed current continuously or in a pulsed mode to the contacts through a probe and the output light will be efficiently coupled through a multi-mode fiber to an optical spectrum analyzer (OSA) where the electroluminescence spectra will be analyzed. The influence of temperature on device performance will be investigated. The temperature of the device will be varied using a thermoelectric (TE) cooler on which the laser will be mounted. The use of interchangeable InGaAs and PbS detectors will allow for a versatile detection system with good sensitivity for emission wavelengths less than  $2.5\mu\text{m}$ .

## 5. Nanoelectromechanically-Actuated Submicron Optical Switches

### Sponsors:

National Science Foundation     Award Number DMR-02-13282

### Project Staff

Reginald E. Bryant, Dr. Gale S. Petrich, and Professor Leslie A. Kolodziejski

The demand for speed, access, and data delivery over the Internet initially fueled the development of photonic integrated chip (PIC) technology. PIC technology held the promise of being able to fully leverage underutilized fiber bandwidth while simultaneously increasing network flexibility and efficiency. Incidentally, the inherent qualities of PIC technology envisaged new applications of interest outside of its intended purpose. Specifically, PIC technology found use in so-called lab-on-a-chip applications where evanescent fields are used to interrogate chemical and biological environments for drug discovery, chemical detection and protein characterization. Moreover PIC technology has been identified as the technology to supplant bandwidth-limited copper wires in order to better serve high-speed central processing units (CPU) communication in state-of-the-art computer systems.

A five-generation family of planar, electromechanically-reconfigurable, high-index-contrast optical switches was developed in order to further extend the functionality of PIC technology. A family of mechanical switches were designed to operate at  $\lambda_0=1550\text{nm}$  with desired per device loss of less than 0.3dB, isolation and cross-talk less than -30dB, and bandwidths greater than 100nm. Although these figures of merit for the mechanical optical switches may preclude their use in very large scale integration applications, these optical switches are more than capable of meeting the needs of small scale integration as well as being useful in applications that do not require premium signal-fidelity. On the other hand, these reconfigurable optical switches can be tailored for use in switching fabrics with the monolithic integration of waveguide-based optical amplifiers. Furthermore, switching fabrics that are based on planar electromechanical optical switches, can either be used for broadband switching as-is or for wavelength-specific switching with the monolithic integration of arrayed waveguide gratings.

The family of planar, electromechanically-reconfigurable, high-index-contrast optical switches rely on butt-coupling, directional-coupling, and adiabatic-coupling in order to facilitate the transfer of light between waveguides; electromechanical parallel plate actuators facilitate the spatial reconfiguration of the waveguides. In particular, the in-plane adiabatic directional-coupler switch (generation 5 of the family of switches) features electromechanical switching for a variety of waveguide-based devices (e.g., lasers, biologically-functionalized waveguides) without imposing design restrictions (e.g., doping levels, material alloy compositions) on the waveguide structure. In general, all of the generations of switches can be implemented in a variety of material systems with the only requirement being that the chosen material system has a high-index of refraction ( $n\sim 3$ ).

## 6. Mid-IR Light Sources

### Sponsors:

Alfaisal University     Award Number: 014-767-001

### Project Staff

Peichun (Amy) Chi, Dr. Gale S. Petrich, and Professor Leslie A. Kolodziejski

Interest in light sources emitting in the mid-infrared (MIR) wavelength region (2-5 $\mu\text{m}$ ) is growing due to their use in telecommunication and molecular spectroscopy applications. The former takes advantage of an atmospheric transparent window for MIR wavelengths and the latter due to the strong absorption lines of certain carbon-based and polluting gases. The goal of this project is to fabricate a room temperature, continuous wave, antimony-based laser and use this light source in photo-acoustic spectroscopy system for the detection of trace amounts of volatile impurities in petrochemicals.

For quantum well semiconductor lasers, the wavelength is a function of well width, valence and conduction band offsets, carrier effective mass, and the band gap of the quantum well material. Hence, simulations were performed to determine the quaternary alloy compositions and the relative thicknesses of the quantum wells and barriers in order to achieve the desired wavelength. Apart from the active region, adjusting the cladding layer thickness also allows the optical mode, the confinement factor and loss to be varied. The following laser structure (see Figure 1) provides emission near 2.3 $\mu\text{m}$  based on MATLAB simulations:

A n-type GaSb buffer, a 100nm-thick n-type layer graded from GaSb to  $\text{Al}_{0.9}\text{Ga}_{0.1}\text{As}_{0.07}\text{Sb}_{0.93}$ , a 2 $\mu\text{m}$  thick  $\text{Al}_{0.9}\text{Ga}_{0.1}\text{As}_{0.07}\text{Sb}_{0.93}$  n-type cladding layer, an 800nm active region containing multiple  $\text{In}_{0.35}\text{Ga}_{0.65}\text{As}_{0.11}\text{Sb}_{0.89}$  quantum wells that are 10.5nm-thick and 1.4% compressively strained, barriers and separate confinement layers that are composed of  $\text{Al}_{0.25}\text{Ga}_{0.75}\text{As}_{0.02}\text{Sb}_{0.98}$ , a 2 $\mu\text{m}$  thick  $\text{Al}_{0.9}\text{Ga}_{0.1}\text{As}_{0.07}\text{Sb}_{0.93}$  p-type cladding layer, a 100 nm-thick p-type layer graded from  $\text{Al}_{0.9}\text{Ga}_{0.1}\text{As}_{0.07}\text{Sb}_{0.93}$  to GaSb, and finally 300 nm-thick p+- GaSb cap layer.

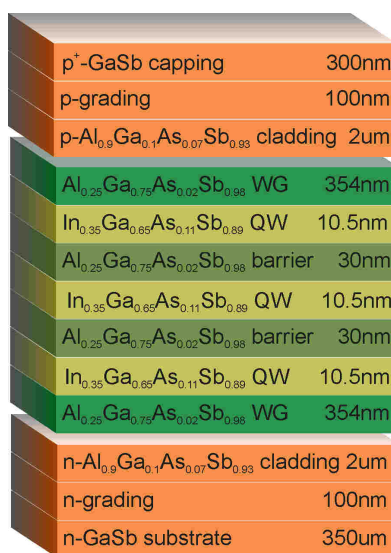


**Figure 1)** A schematic of a laser structure with an emission wavelength near 2.3  $\mu\text{m}$

Currently, the molecular beam epitaxial growth conditions that are necessary to grow the aforementioned laser structure are being determined. The MBE growth conditions include the substrate temperature, V/III flux ratio, and growth rate. Each quaternary film will be characterized after growth using the high resolution x-ray diffractometer in the Center for Material Science and Engineering (CMSE) to determine the layer composition, the layer thickness, the surface roughness, and lattice relaxation. The surface roughness can also be determined by using an atomic force microscope (AFM) and/or a scanning electron microscope (SEM); the composition will also be confirmed by Auger Electron Spectroscopy (AES). The MBE growth conditions can be optimized by measuring the full-width at half-maximum of the photoluminescence and/or x-ray diffraction peaks. Optical and electrical properties will be measured by photoluminescence, ellipsometry and Hall measurements.

## Publications

### Journal Articles, Published

#### Journal Articles, Submitted

Ta-Ming Shih, Andre Kurs, Marcus Dahlem, Gale Petrich, Marin Soljacic, Erich Ippen, Leslie Kolodziejski, Katherine Hall, and Morris Kesler, *Supercollimation in Photonic Crystals Composed of Silicon Rods* Submitted to Applied Physics Letters, (2008)

#### Meeting Papers, Published

Ta-Ming Shih, Marcus Dahlem, Andre Kurs, Gale Petrich, Marin Soljacic, Erich Ippen, Leslie Kolodziejski, Katherine Hall, and Morris Kesler, "Supercollimation in Photonic Crystals Composed of Nano-Scale Silicon Rods" *Lasers and Electro-Optics, 2008 and 2008 Conference on Quantum Electronics and Laser Science. CLEO/QELS 2008. Conference on 4-9 May 2008* Page(s):1 - 2

Dominik Pudo, Hyunil Byun, Juliet Gopinath, Gale S Petrich, Erich P Ippen, Franz X Kaertner, Leslie A. Kolodziejski, "Nonlinear phase response of a saturable Bragg reflector for modulation depth control" *Lasers and Electro-Optics, 2008 and 2008 Conference on Quantum Electronics and Laser Science. CLEO/QELS 2008. Conference on 4-9 May 2008* Page(s):1 - 2

#### Theses

O. Shamir, *Development of Ultra-Broadband Modulators*, M. Eng. Thesis, Department of Electrical Engineering and Computer Science, MIT, 2008.

T-M. Shih, *Super-collimation in a Rod-based Photonic Crystal*, M. S. Thesis, Department of Electrical Engineering and Computer Science, MIT, 2007.

N. Jovanović, *Microstructured Tungsten Thermophotovoltaic Selective Emitters*, Ph. D. Thesis, Department of Electrical Engineering and Computer Science, MIT, 2008

R. Williams, *Photonic Integrated Circuits for Optical Logic Applications*, Ph. D. Thesis, Department of Material Science and Engineering, MIT, 2007

